Journal of Chromatography A 1645 (2021) 462122

Contents lists available at ScienceDirect

Journal of Chromatography A

journal homepage: www.elsevier.com/locate/chroma

Silver (I)-dimercaptotriazine functionalized silica: A highly selective liquid chromatography stationary phase targeting unsaturated molecules

Sian Liao[a,1], James T. Dillon[a,1], Cancan Huang[a], Ewerton Santos[b], Yongsong Huang[b,*]

[a] Department of Chemistry, Brown University, 324 Brook Street, Providence, Rhode Island 02912, USA
[b] Department of Earth, Environmental and Planetary Sciences, Brown University, 324 Brook Street, Providence, Rhode Island 02912, USA

ARTICLE INFO

Article history:
Received 14 February 2021
Revised 25 March 2021
Accepted 28 March 2021
Available online 30 March 2021

Keywords:
Silver-thiolate chromatography
Silver(I)-dimercaptotriazine
Silver ion chromatography
Van't Hoff plots
Lipid analysis

ABSTRACT

Silver(I)-mercaptopropyl (Ag-MP) functionalized silica gel has demonstrated its effectiveness in separating various unsaturated organic compounds including unsaturated fatty acid ethyl esters (FAEEs), triglycerols (TAGs) and long-chain alkyl ketones (alkenones). While Ag-MP stationary phase displays many advantages over the conventional silver ion-impregnated silica gel (e.g., stability, high recovery, etc.), potential drawbacks of Ag-MP include relatively low retentions for unsaturated molecules, which could limit chromatographic resolutions under certain circumstances. In this study, we evaluate a new silver-thiolate stationary phase: silver(I)-dimercaptotriazine (Ag-DMT) functionalized silica gel targeting the separation of unsaturated compounds. We show Ag-DMT affords substantially higher retention factors, peak resolutions and capacities for TAGs and FAEEs than Ag-MP does. Ag-DMT also yields higher purity eicosapentaenoic acid (EPA) from fish oil FAEE mixtures than Ag-MP. In addition, Ag-DMT resolves double bond positional and *cis/trans*-isomers of $C_{18:1}$ fatty acid methyl esters (FAMEs) as well as unsaturated methyl/ethyl alkenones with different number of double bonds. Based on van't Hoff plots, enthalpy changes during the adsorption of unsaturated FAEEs onto Ag-DMT are ~2 times higher than those on Ag-MP. Such difference may be attributed to the stronger electron-withdrawing effect of the thiol group on DMT, which results in more positively charged silver ions hence greater interactions with unsaturated molecules. The stronger interaction between double bonds and Ag-DMT is further corroborated by density-functional theory (DFT) calculations. Ag-DMT shows its high stability for repeated uses in the separation of TAGs over 319 runs, with peak resolutions decreasing by $< 3\%$. Collectively, our data demonstrate the exceptionally high efficiency of Ag-DMT column for separating unsaturated molecules.

1. Introduction

Developed in the early 1960s, silver ion chromatography has been a frequently used and unique technique specifically targeting the separation of unsaturated organic compounds, which is based on the reversible interaction between silver ions and unsaturated bonds [1,2]. However, one major issue of the silver ion chromatography is the stationary phase instability [3,4]. There are three aspects of the instability: 1) the light-induced reduction of silver ion into silver metal, which does not interact with double bonds; 2) the high redox potential of silver ions, which threatens oxidation of olefins and results in potentially low recovery of target compounds during the chromatographic separation; and 3) the weak electrostatic interaction between silver ions and the surface Si-OH groups, leading to the relatively high mobility of the stationary phase. Specifically, under the influence of polar mobile phases and analytes containing multiple double bonds (hence strong affinity to silver ions), silver ions may become partially mobile and even leak from the stationary phase, decreasing the separation performance and causing damage to detectors when used in high-performance liquid chromatography (HPLC) [4–6].

We have demonstrated that the silver ion (I) can be readily stabilized via a covalent bond with a thiol moiety on mercaptopropyl group linked to silica gel [6–10]. The resulting silver(I)-mercaptopropyl (Ag-MP) stationary phase is highly effective for separating various unsaturated organic compounds including fatty acid ethyl esters (FAEEs) [7], triglycerols (TAGs) [6] and long-chain alkyl ketones (also called alkenones, a class of important geochemical biomarkers produced by Isochrysidales, an order of haptophyte algae in ocean and lakes) [8]. Ag-MP features long-term stability,

---

[*] Corresponding author.
E-mail address: yongsong_huang@brown.edu (Y. Huang).
[1] These authors contributed equally.

https://doi.org/10.1016/j.chroma.2021.462122
0021-9673/

high reproducibility, strong light stability, high compound recovery and mass spectrometer compatibility [5]. However, despite all these advantages mentioned above, its relatively low retentions for unsaturated molecules could limit resolutions for different compounds containing the same number of double bonds. For example, Ag-MP cannot resolve eicosapentaenoic acid (EPA) ($C_{20:5}$) from heneicosapentaenoic acid (HPA, $C_{21:5}$) and docosapentaenoic acid (DPA, $C_{22:5}$). Such co-elution limits the maximal purity of EPA to ~95% when HPLC equipped with Ag-MP is used for fish oil fractionations [7].

Here, we introduce a new silver-thiolate stationary phase, silver(I)-dimercaptotriazine (Ag-DMT), for use in HPLC. We demonstrate that Ag-DMT has higher retention factors, peak capacities and resolutions than Ag-MP for unsaturated TAGs and FAEEs. Ag-DMT also provides excellent separation of double bond positional and *cis/trans*-isomers of $C_{18:1}$ fatty acid methyl esters (FAMEs) and alkenones. Thermodynamic properties between Ag-DMT and Ag-MP are compared based on van't Hoff plots established from isocratic HPLC separation of FAEEs. We also evaluate the stability of Ag-DMT in 319 consecutive separations over two months. Theoretical calculations of the binding enthalpy between ethylene and silver site on silver thiolate bond, and bond-dissociation energy of silver thiolate (-S-Ag) bond for Ag-MP and Ag-DMT in gas phase are computed using density-functional theory (DFT) to further compare the two stationary phases.

2. Materials and methods

2.1. Materials

All solvents were HPLC grade from Fisher Scientific (USA). Silver nitrate (>99%), HNO_3 (65%, w/v) and HF (40%, w/v) were purchased from Sigma-Aldrich (USA). 3-mercaptopropyl functionalized silica (3 μm particle size, 60 Å pore size. 1.27 mmol/g molecular loading) and dimercaptotriazine functionalized silica (3 μm particle size, 60 Å pore size. 0.58 mmol/g molecular loading), and plain silica gel for sample purification (230-400 mesh, 40-63 μm, 60 Å pore size) were obtained from Silicycle Inc. (Canada). Fatty acid methyl esters (FAMEs) were obtained from Restek (USA). A mixture of FAMEs was comprised of methyl stearate ($C_{18:0}$, methyl ester of fatty acid with 18 carbon atoms and zero C=C bond) (20%, w/w), methyl linoleate ($C_{18:2}$) (20%, w/w) and the following methyl octadecenoate ($C_{18:1}$) isomers (60%, w/w): *trans*-Δ^6 (8%, w/w), *trans*-Δ^9 (10%, w/w), *trans*-Δ^{11} (12%, w/w), *cis*-Δ^6 (8%, w/w), *cis*-Δ^9 (10%, w/w), *cis*-Δ^{11} (12%, w/w) (numbering from the ester group). Fish oil samples were purchased from Whole Foods Market. For fatty acid residuals in TAGs, we used the following abbreviations: S, stearic acid ($C_{18:0}$); O, oleic acid ($C_{18:1}$); L, linoleic acid ($C_{18:2}$); Ln, linolenic acid ($C_{18:3}$); P, palmitic acid ($C_{16:0}$). Alkenone samples were extracted from sediments of Lake Braya Sø, an oligohaline lake (1-3 psu) located in the Søndre Strømfjord region of west Greenland [11].

2.2. Preparation of fatty acid ethyl esters (FAEEs)

Fatty acid ethyl esters (FAEEs) were prepared by an acid-catalyzed esterification in ethanol. An ethanol/acetyl chloride solution (95:5, v/v) was prepared by drop-wise addition of acetyl chloride to ethanol, producing catalytic amount of HCl. Approximately 50 mg of fish oil was dissolved in a mixed solution containing 250 μL toluene and 250 μL ethanol/acetyl chloride, and heated to 70°C for 8 hours. The reaction was cooled to room temperature. Then 1 mL hexane and 1mL NaCl solution (5%, w/w) were added to the reaction mixture and shaken vigorously for 3 minutes. The organic phase was extracted three times with 3 × 1 mL hexane. The combined extracts were evaporated to dryness under N_2, dissolved in 0.50 mL hexane and further cleaned by silica gel. The silica gel column (prepared in a glass pipette, ~1.5 g SiO_2) was loaded with crude FAEE samples and eluted with hexane (4 mL) and dichloromethane (4 mL). FAEEs were in the dichloromethane fraction. The dichloromethane fraction was evaporated to dryness and dissolved in heptane (1 mL). Average yield of this reaction was around 85%.

2.3. HPLC column preparations and determination of the silver loading

Silver(I)-thiolate stationary phases used in this work were prepared from 3-mercaptopropyl or dimercaptotriazine functionalized silica using procedures established previously [5]. Briefly, 3-mercaptopropyl/dimercaptotriazine bonded silica (1.6 g) was suspended in 25 mL of water/methanol (1:1, v/v). A small excess of silver nitrate (~1.2 eq.) was added. The slurry was stirred at room temperature for 2 hours. The product was then filtered and washed with water (50 mL) and methanol (50 mL) three times to remove excess $AgNO_3$ and HNO_3, then dried overnight at 60°C. The obtained silver(I)-mercaptopropyl/dimercaptotriazine functionalized silica gel was packed into a stainless steel HPLC column (150 mm x 3.0 mm i.d.) at 8,000 psi (~551 bar) by Princeton Chromatography (NJ, USA) [6,7].

To determine the silver loading of silver(I)-dimercaptotriazine (Ag-DMT) (3 μm particle size) used in HPLC column, Ag-DMT was digested with HF and HNO_3 based on reported procedures [12–14]. ~20 mg Ag-DMT was added into a round-bottom Teflon vial containing 4 mL acid mixture (75% HNO_3, 25%HF, v/v). The suspension was stirred at 40°C for 3 h to obtain a clear solution. The solution was evaporated to dryness at 100°C, and then re-dissolved with 4 mL HNO_3 (18%, w/v) by heating at 40°C for 3h and diluted into 2% HNO_3 solution before ICP-MS analysis. The silver loading for Ag-DMT (3 μm) was determined to be 5.0% (silver weight percentage relative to Ag-DMT silica).

2.4. HPLC-APCI-MS conditions

HPLC system consisted of a binary pump, thermostatted column compartment and autosampler (Agilent 1200 series), coupled to a quadrupole LC/MS detector (Agilent 6130 series) equipped with an atmospheric-pressure chemical ionization (APCI) probe. The system was controlled by Agilent OpenLab CDS ChemStation software. All experiments described in this work were performed with silver(I)-dimercaptotriazine column (150 mm x 3.0 mm i.d., 3 μm) or silver(I)-mercaptopropyl column (150 mm x 3.0 mm i.d., 3 μm). The flow rate was 0.5 mL/min during the whole experiment.

The following conditions for the APCI probe were used for analyzing molecules across all mobile phases and temperatures examined: vaporizer temperature (350-400°C), nebulization pressure (50-60 psig), drying gas flow (5.0-6.0 L/min), drying gas temperature (250-300°C), corona current (5.0 µA) and capillary voltage (3500 V). Scanning mass ranges are: FAME and FAEEs, 225-400 *m/z*; TAGs, 500-1000 *m/z*; alkenones, 225-750 *m/z*. Ionization by APCI yielded $[M+H]^+$ parent ions for identifications.

2.5. Theoretical calculations of modeled structures of Ag-MP and Ag-DMT in gas phase

Modeled structures of Ag-MP and Ag-DMT in gas phase were studied by B3LYP density functional [15] with LANL2DZ basis set [16] using Gaussian 09 software package [17]. The B3LYP/LANL2DZ method was reported to yield highly consistent binding enthalpy of Ag^+-C_2H_4 with experimental values [18]. After geometry optimizations, binding enthalpy of ethylene and the bond-dissociation energy of -S-Ag bond into -S$^-$ and Ag$^+$ in gas phase were calculated for Ag-MP and Ag-DMT. The optimized structures were rendered using Avogadro [19].

2.6. Data analysis

Sample peak capacity (PC) was calculated from the retention time of the first peak (t_a), last peak (t_z) and average peak width (W_{avg}) using Eq. (1) [20]:

$$PC = \frac{t_z - t_a}{W_{avg}} \tag{1}$$

Van't Hoff plots provide a convenient method to study the thermodynamic properties of Ag-MP and Ag-DMT stationary phases. Enthalpy and entropy changes during the adsorption of analytes onto the stationary phases can be obtained through a correlation between retention factors of analytes under isocratic elution and different temperatures, using Eq. (2) [21,22]:

$$lnk(A) = \frac{\Delta S^0}{R} + ln\Phi - \frac{\Delta H^0}{R}\left(\frac{1}{T}\right) \tag{2}$$

where $k(A)$ is the retention factor for peak A, T is the temperature, R is the gas constant, ΔS^0 and ΔH^0 are the changes of standard entropy and standard enthalpy during the adsorption of analyte onto the stationary phase, respectively, and Φ is the phase ratio (stationary phase volume divided by mobile phase volume). Isocratic elution is necessary because values of phase ratios and the equilibriums of analytes from the mobile phase to stationary phase are closely related to the mobile phase compositions (hence gradient elution adds additional variables, making it difficult to obtain values of enthalpy and entropy changes). A linear correlation between lnk and $\frac{1}{T}$ is expected, if the interaction mechanism remains unchanged during the adsorption of analytes under different temperatures. Temperature-dependence of ΔS^0, ΔH^0 and Φ could also influence the linearity of van't Hoff plots. However, such temperature-dependence, which has only been reported in a limited number of studies [23,24], is thus uncommon.

Influence of entropy and enthalpy values on the selectivity α_{A-B} was calculated using Eq. (3) deduced from Eq. (2):

$$ln\alpha_{A-B} = \frac{\Delta\Delta S^0}{R} + \frac{\Delta\Delta H^0}{RT} \tag{3}$$

where $\Delta\Delta S^0 = \Delta S^0_B - \Delta S^0_A$ and $\Delta\Delta H^0 = \Delta H^0_A - \Delta H^0_B$. ΔS^0_A and ΔH^0_A are the changes of standard entropy and enthalpy for the first peak A. ΔS^0_B and ΔH^0_B are the changes of standard entropy and enthalpy for the second peak B.

3. Results and discussion

3.1. Comparison of retention factors, peak resolutions and peak capacities between Ag-DMT and Ag-MP

3.1.1. Separations of fish oil FAEEs

Ag-DMT stationary phase displays much higher retention factors than Ag-MP in the separation of fish oil FAEEs (e.g., retention factor of $C_{16:4}$ FAEE increases by 440%), indicating substantially stronger interactions between double bonds and Ag-DMT stationary phase (Fig. 1). Ag-DMT also yields higher peak resolutions and peak capacities, with the greatest increase in peak resolution between peak 4a ($C_{16:4}$) and peak 5b ($C_{21:5}$) by 667%, and an overall increase of peak capacity by ~195%. The separation of unsaturated molecules in both stationary phases is primarily based on degrees of unsaturation, as expected. However, further separation of molecules with the same number of double bonds but different carbon chain lengths or double bond positions is observed for Ag-DMT, but not Ag-MP (Fig. 1b). With Ag-DMT stationary phase, FAEEs with shorter chain lengths are in general less retained (e.g., $C_{16:2}$ elutes faster than $C_{18:2}$, $C_{16:3}$ elutes faster than $C_{18:3}$, $C_{16:4}$ elutes faster than $C_{18:4}$ and $C_{20:4}$, and $C_{20:5}$ elutes faster than $C_{21:5}$ and in turn $C_{22:5}$). Such elution orders are opposite to those observed in the separation of fatty acid derivatives using silver ion silica gel column, when molecules with longer chain lengths are less retained [3,25]. The difference in the elution orders between Ag-DMT and silver ion silica gel column can be explained by: 1) exposed or partially exposed silanol groups in silver ion column have weaker interactions with less polar, longer carbon chain length molecules [3,25,26]; 2) the large dimercaptotriazine group in Ag-DMT displays some reversed-phase chromatographic interaction (van der Waals force between alkyl chains and dimercaptotriazine groups) with FAEEs, with greater retention for those with longer carbon chain lengths; and 3) the steric effect of large dimercaptotriazine groups prevents interaction of FAEEs with underivatized silanol groups on the surface of the silica.

EPA, an omega-3 polyunsaturated fatty acid of great commercial value, is thought to serve multiple positive roles in human bodies such as cognitive and behavioral function and cardiovascular health [27]. There is an increasing demand of high-purity EPA for pharmaceutical applications, such as controlling TAG level in patients with hypertriglyceridemia [28]. The presence of other fatty acids (e.g., DPA) may reduce the clinical efficiency of EPA [29]. In a pilot exploration for the production of high-purity EPA at commercial scale, silver ion-impregnated silica gel column partially resolved DPA from EPA and yielded ~90% pure EPA [30]. However, repeated use of silver ion-impregnated silica gel column could lead to significant silver contamination in the EPA product. The cost of production is also enhanced due to the need of frequent regeneration of silver ion-impregnated column (regeneration, as a result of silver ion leaching, is needed after ~50 cycles to maintain the separation performance) [30].

Ag-MP is characterized by the exceptionally high stability [5,6], but the retention for unsaturated compounds is relatively low. For example, retention factors for FAEEs with 1 to 6 double bonds range from 0.5 to 2.3 (Fig. 1a). This is advantageous for reducing the time needed for separations, but could be problematic for resolving compounds with small structural differences. In our previously reported separation with Ag-MP stationary phase, the isolated EPA fraction contained impurities of HPA and DPA as revealed by subsequent gas-chromatography-mass spectrometry (GC-MS) analysis [7]. With Ag-DMT, HPA and DPA are fully resolved from EPA (Fig. 1b). Notably, EPA and tetra-/hexa-unsaturated FAEEs are also better resolved (Fig. 1b, resolutions increase by ~36% between EPA and tetra-unsaturated FAEEs, and ~38% between EPA and hexa-unsaturated FAEEs than Ag-MP does). Overall, our results indicate Ag-DMT is an excellent stationary phase for the purification of high-grade EPA for pharmaceutical applications.

3.1.2. Separations of TAGs

TAGs are common fat molecules composed of three variably unsaturated fatty acid residuals esterified to a glycerol. They are widely distributed in meats and vegetables, playing an important role in metabolism [31]. Similar to the separation of FAEEs, Ag-DMT shows stronger retentions, higher peak resolutions and greater peak capacities for TAGs than Ag-MP does (Fig. 2). For example, the resolution between di-unsaturated peak 2a (LPP, SOO, SSL, PPL) and tri-unsaturated peak 3b (OOO and SOL) increases by 228%, and overall peak capacity increases by 90%, when Ag-MP is replaced with Ag-DMT. Ag-DMT provides additional separation based on the number of carbon atoms and double bond positions, but Ag-MP does not. Similar to the separation of FAEEs, TAGs with lower carbon numbers are less retained by Ag-DMT (Fig. 1b), opposite to the traditional silver ion silica gel column [26].

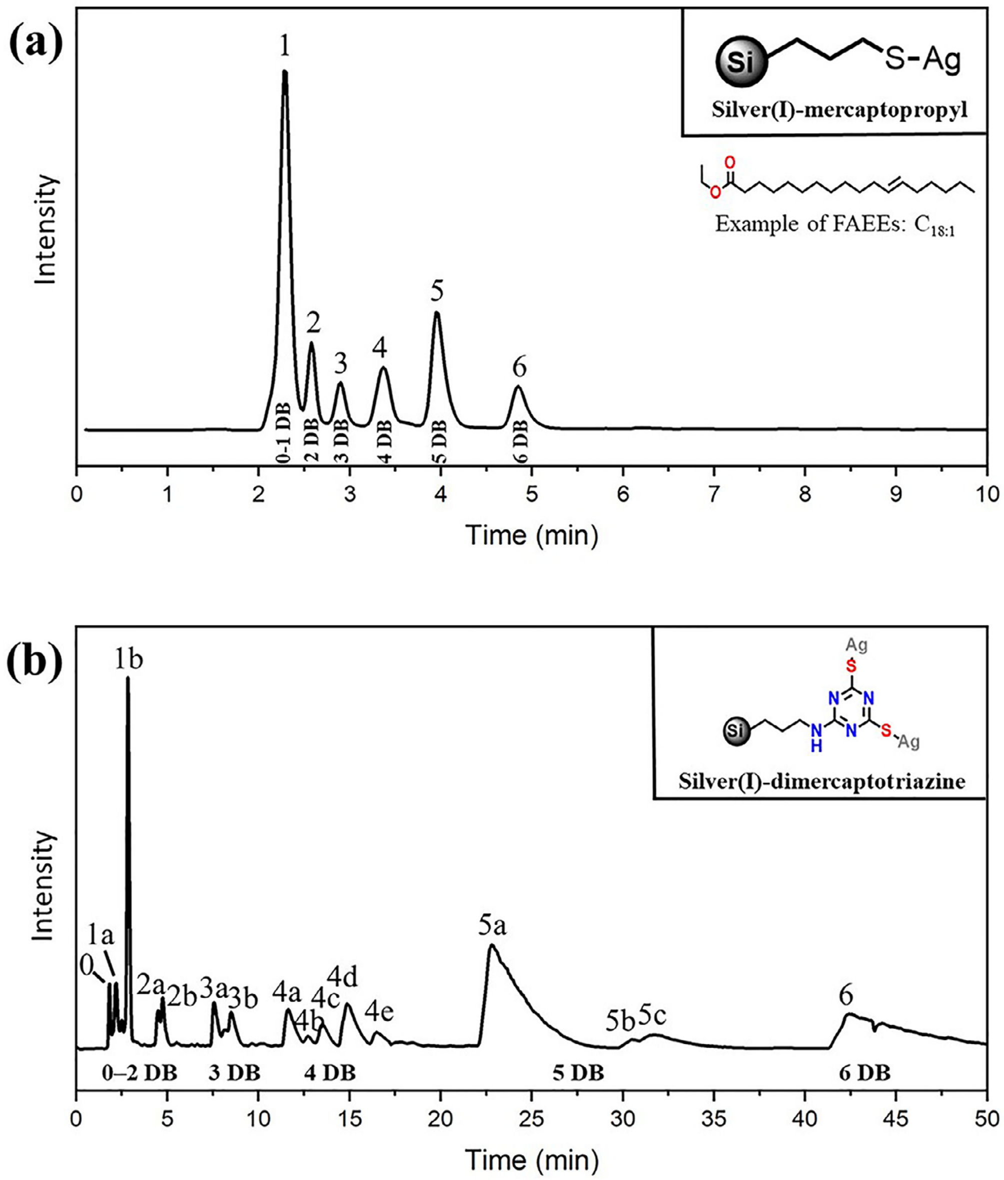

Fig. 1. Total ion chromatograms of fish oil FAEEs. The separations were carried out using HPLC-APCI-MS with an isocratic elution of 95% hexane and 5% acetone using (a) Ag-MP and (b) Ag-DMT at 15°C. In chromatogram (a), 1: $C_{14:0}$, $C_{16:0}$, $C_{16:1}$, $C_{17:1}$ and $C_{18:1}$, 2: $C_{16:2}$ and $C_{18:2}$, 3: $C_{16:3}$ and $C_{18:3}$, 4: $C_{16:4}$, $C_{18:4}$ and $C_{20:4}$, 5: $C_{20:5}$, $C_{21:5}$ and $C_{22:5}$, 6: $C_{22:6}$. In chromatogram (b), 0: $C_{14:0}$ and $C_{16:0}$, 1a: $C_{16:1}$ and $C_{17:1}$, 1b: $C_{18:1}$ and $C_{16:1}$, 2a: $C_{16:2}$, 2b: $C_{18:2}$, 3a: $C_{16:3}$, 3b: $C_{18:3}$, 4a: $C_{16:4}$, 4b: $C_{18:4}$, 4c: $C_{20:4}$, 4d: $C_{18:4}$, 4e: $C_{20:4}$, 5a: $C_{20:5}$, 5b: $C_{21:5}$, 5c: $C_{22:5}$, 6: $C_{22:6}$. Numbers above each peak denote the number of double bonds in the molecule.

Traditionally, TAGs can be analyzed by high-temperature gas chromatography (HT-GC) [32–34], reversed-phase HPLC [35,36] and silver ion HPLC [3,37,38]. HT-GC separates TAGs based on the number of carbon atoms and/or unsaturation degrees with resolutions comparable to TAGs analyzed by reversed-phase HPLC [34–39]. The main challenges of HT-GC in the analysis of TAGs include the thermal-degradation of polyunsaturated TAGs, fast column deterioration and limited resolutions for double bond positional isomers [33,34]. Reversed-phase HPLC can readily separate TAGs with high resolutions based on partition number ($PN = CN - 2DB$, where CN is the number of total carbon atoms and DB is the number of double bonds) [32,40], but could add unnecessary complexities in separations aimed at characterizing double bonds (number, position and geometry) [41]. Importantly, neither GC nor reversed-phase HPLC is commonly used for the preparative purpose of lipids, due to the low loading capacity (low solubility of lipids in the starting polar solvents in reversed-phase HPLC). Silver ion HPLC provides separation mainly based on unsaturation degrees and is widely used as a preparative method for the fractionation of TAGs [32,34]. It yields easy-to-interpret chromatograms for characterizing double bonds, but the leaching silver ions (especially for silver ion-impregnated HPLC column) are problematic. The stability problem is partially solved with the development of cation-exchange silver ion HPLC column, which was reported to yield reproducible results in the analysis of TAGs after > 70 injections over four weeks [3,42]. Notably, fast column deterioration could still occur in practice for the cation-exchange silver ion column after relatively small number of runs [3,43].

3.2. Selectivity towards double bond positional and *cis/trans*-isomers of FAMEs

Fig. 3 shows the separation of double bond positional and *cis/trans*-isomers of $C_{18:1}$ FAMEs with the Ag-DMT stationary phase. For $C_{18:1}$ FAMEs, *trans*-isomers (*trans*-Δ^6, *trans*-Δ^9, *trans*-Δ^{11}) are less retained than *cis*-isomers (*cis*-Δ^6, *cis*-Δ^9, *cis*-Δ^{11}), consistent

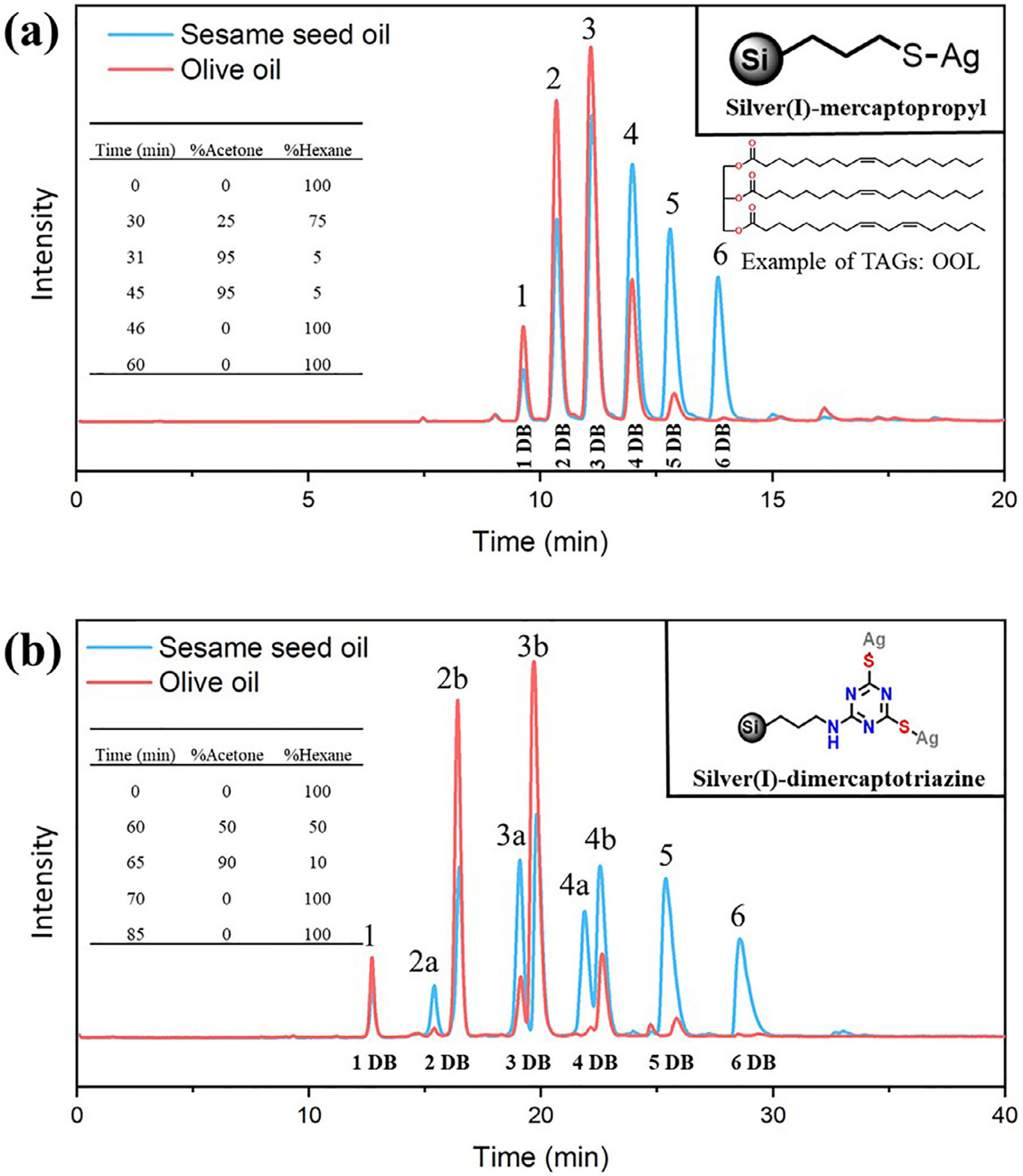

Fig. 2. Total ion chromatograms of sesame seed oil (blue) and olive oil (red). The separations were carried out using HPLC-APCI-MS equipped with (a) Ag-MP and (b) Ag-DMT at 25°C. Peaks of TAGs were tentatively assigned based on fragmented ions and TAGs already identified (relative position of fatty acid residuals on the glycerol chain was uncertain) [39]. In chromatogram (a), 1: OPP, SOP and SSO, 2: LPP, SOO, SSL, PPL, OOP and SLP, 3: OOO, SOL and POL, 4: PLL, SLL and OOL, 5: OLL and OOLn, 6: LLL and OLLn. In chromatogram (b), 1: OPP, SOP and SSO, 2a: LPP, SOO, SSL and PPL, 2b: OOP and SLP, 3a: POL, 3b: OOO and SOL, 4a: PLL and SLL, 4b: OOL, 5: OLL and OOLn, 6: LLL and OLLn. Numbers above each peak denote the number of double bonds in the molecule.

with observations from silver ion columns [3,44]. This can be readily explained by the greater steric effect of *trans*-isomers than *cis*-isomers of FAMEs. Ag-DMT also affords high resolutions among *trans*-Δ^6/*cis*-Δ^6 ($R_s = 8.5$), *trans*-Δ^9/*cis*-Δ^9 ($R_s = 16.8$), and *trans*-Δ^{11}/*cis*-Δ^{11} ($R_s = 10.7$). The elution order of double bond positional isomers follows Δ^6-$C_{18:1}$ < Δ^9-$C_{18:1}$ < Δ^{11}-$C_{18:1}$, for both *cis*- and *trans*-isomers. Double bond positional isomers of $C_{18:1}$ FAME are resolved for *trans*-Δ^6/*trans*-Δ^9 ($R_s = 5.7$) and *cis*-Δ^6/*cis*-Δ^9 ($R_s = 7.7$). Partial coelution is observed for *trans*-Δ^9/*trans*-Δ^{11} ($R_s = 0.5$) and *cis*-Δ^9/*cis*-Δ^{11} ($R_s = 0.3$). The elution order of positional isomers on Ag-DMT is again opposite to that on silver ion column (Δ^{11}-$C_{18:1}$ < Δ^9-$C_{18:1}$ < Δ^6-$C_{18:1}$) [3,45]. With silver ion column, Nikolova-Damyanova et al. (1996) proposed a dual interaction model where both C=C and C=O bonds in mono-unsaturated fatty acid could interact with single silver sites [45]. Δ^6-$C_{18:1}$ forms a more stable coordination complex with silver ion than Δ^{11}-$C_{18:1}$ does, hence the former is more retained in silver ion HPLC [45]. The inverse elution order with Ag-DMT may be related to the spatial arrangement of the two adjacent silver thiolate groups on the dimercaptotriazine: isomers with C=C and C=O further apart from each other (e.g., Δ^{11}-$C_{18:1}$) would form more stable complexes with silver sites.

Separation of double bond positional and *cis*/*trans*-isomers of mono-unsaturated fatty acids was previously mainly achieved with GC and silver ion HPLC [46–50]. GC features high resolution, and ability to determine double bond positions when coupled to mass spectrometry after converting fatty acids into certain derivatives (e.g., 4,4-dimethyloxazolidine (DMOX) derivatives) [46]. Interestingly, the elution order of FAMEs in gas chromatography is similar to that of Ag-DMT column (*trans*-isomers elute faster than *cis*-isomers, Δ^6-$C_{18:1}$ < Δ^9-$C_{18:1}$ < Δ^{11}-$C_{18:1}$) [51]. On the other hand, silver ion chromatography is more frequently used for prepara-

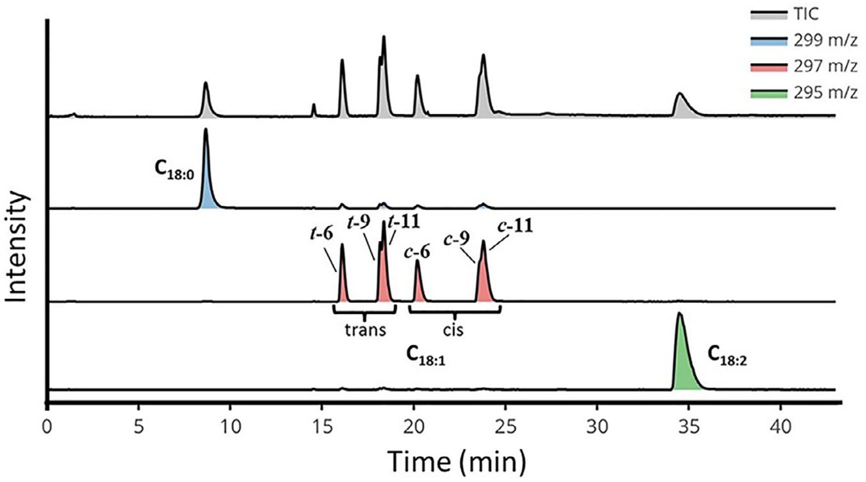

Time (min)	0	60	61	70	71	85
%Acetone	0	5	100	100	0	0
%Hexane	100	95	0	0	100	100

Fig. 3. Total ion chromatogram of FAME mixture samples (composed of $C_{18:0}$, $C_{18:2}$ and $C_{18:1}$ *cis/trans-* and positional isomers). The separation was carried out using HPLC-APCI-MS equipped with Ag-DMT at 25°C.

tive purpose before further structural analysis with GC. Here we show that Ag-DMT HPLC operated under normal phase conditions can also be used in the separation of double bond positional and *cis/trans*-isomers with silver sites stabilized by thiol groups.

3.3. Selectivity towards alkyl structures of alkenones and influence of mobile phase conditions

Alkenones are a class of polyunsaturated long-chain ketones produced by Isochrysidales, an order of haptophyte algae [52,53]. Because of the strong linear response between their unsaturation degrees and environmental temperature, alkenones are of particular interest to paleoclimatologists and paleoceanographers, and have been widely used for paleo-sea surface temperature (SST) reconstructions in the past 40 years [52]. Recently, alkenones have also been explored as components of cosmetics [54] and biofuels for jet engines [55].

We observe an interesting phenomenon in the separation of alkenones with Ag-DMT. Besides the separation based on the number of double bonds, additional separation between methyl and ethyl alkenones is observed (Fig. 4). For alkenones with same number of C=C double bonds, ethyl alkenones elute faster than methyl alkenones. Similar phenomenon was also observed in the reported separation of alkenones with Ag-MP stationary phase [8]. Methyl and ethyl alkenones have the same double bond positions (e.g., double bond positions for tetra-unsaturated $C_{38:4}$Me and $C_{38:4}$Et alkenones are the same Δ^7, Δ^{14}, Δ^{21} and Δ^{28}, numbering from the carbonyl carbon) [8]. Therefore, the earlier elution of ethyl alkenones indicates that C=O bond in ethyl alkenones may have a weaker interaction with silver site than that in methyl alkenones, probably due to steric interference.

$C_{38:2}$Et alkenone co-elutes with unknown compounds when acetone gradient increases at 0.50%/min. The unknown compounds are fully resolved from alkenones with slower rate of solvent polarity increase (0.33% acetone increase/min) (Fig. 4). Because of the high retention factors of alkenones with Ag-DMT (retention factors range from 7.1 to 10.1 when acetone gradient increases at 0.50%/min, 9.0 to 13.2 at 0.33%/min, and 13.9 to 21.3 at 0.17%/min), resolutions for pairs of alkenones do not change significantly with decreasing solvent polarity. Specifically, when acetone gradient decreases from 0.5% to 0.17%/min, resolutions increase only slightly for pairs of ethyl alkenones ($R_s = 5.2 \rightarrow 6.9$ between di- and tri-unsaturated ethyl alkenones, $R_s = 3.9 \rightarrow 4.3$ between tri- and tetra-unsaturated ethyl alkenones). In contrary, the same decrease in acetone gradient reduces the resolutions for pairs of methyl alkenones slightly ($R_s = 5.3 \rightarrow 4.8$ between di- and tri-unsaturated methyl alkenones, $R_s = 3.6 \rightarrow 3.2$ between tri- and tetra-unsaturated methyl alkenones). Peak capacity ($PC =$ 10.9 at both 0.50% acetone/min and 0.17% acetone/min) is almost the same, but peaks show more tailing and broadening at 0.17% acetone/min. Notably, however, unknown compounds are better resolved from alkenones at lower solvent strength (0.17% acetone/min).

3.4. Stability and durability of the Ag-DMT stationary phase

Ag-DMT displays good stability and repeatability in the separation of TAGs during 319 runs over the course of 56 days (Fig. 5). Retention factors decrease slightly in the first 43 runs (e.g., the retention factor of hexa-unsaturated peak 6 decreases by 19%), but change little in the subsequent 276 runs (Fig. S1). Importantly, Ag-DMT column shows little changes in compound resolutions for both pairs of TAGs varied in unsaturation degrees as well as pairs of TAGs with same unsaturation degrees but different number of total carbon atoms/double bond positions (decrease by 2.2% on average, Fig. S2) after the elution with 1.4 L acetone and 5.8 L hexane. The relatively stable resolutions during repeated uses suggest the high stability of Ag-DMT stationary phase, and further corroborate our conclusion [5] that the formation of covalent bond between silver atoms and thiol groups significantly improves the stability of stationary phases while achieving effective separation of unsaturated molecules.

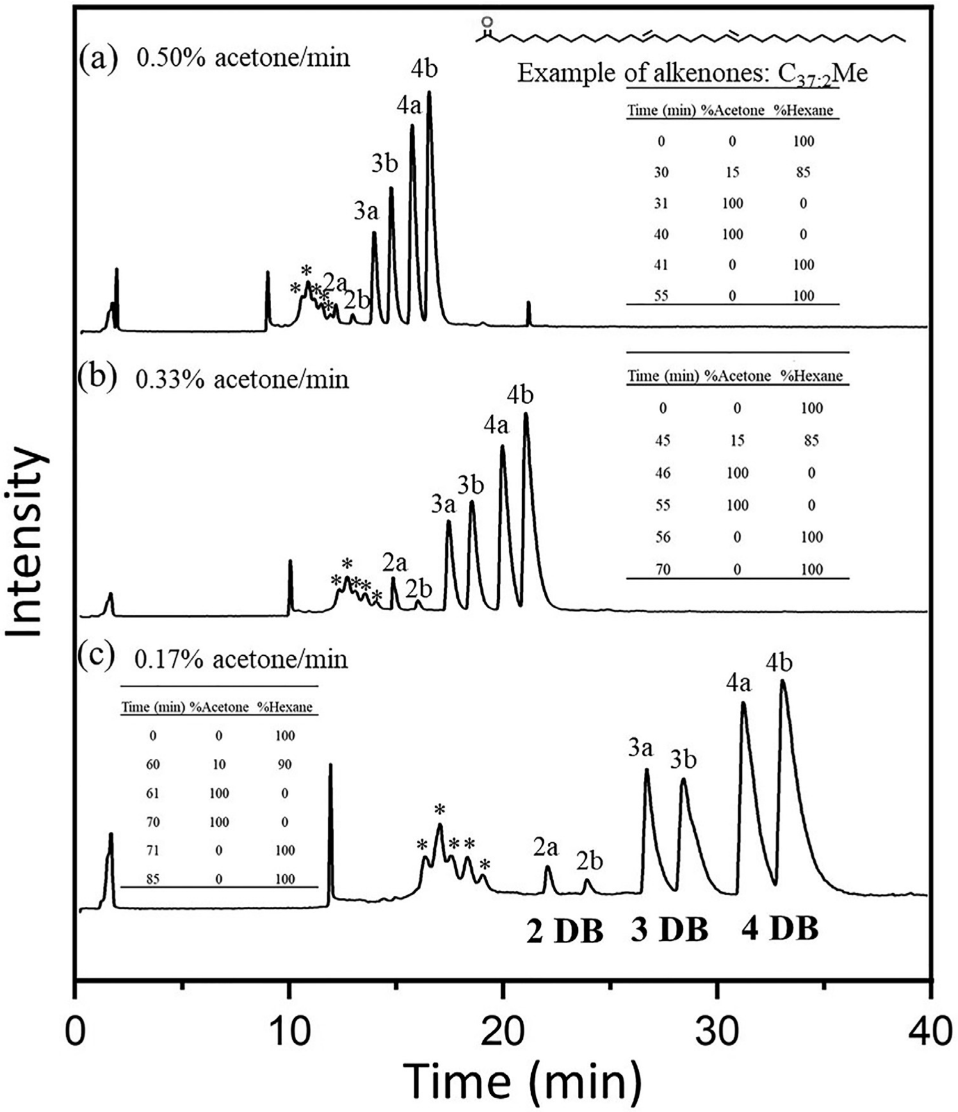

Time (min)	%Acetone	%Hexane
0	0	100
30	15	85
31	100	0
40	100	0
41	0	100
55	0	100

Time (min)	%Acetone	%Hexane
0	0	100
45	15	85
46	100	0
55	100	0
56	0	100
70	0	100

Time (min)	%Acetone	%Hexane
0	0	100
60	10	90
61	100	0
70	100	0
71	0	100
85	0	100

Fig. 4. Total ion chromatograms of alkenones extracted from surface sediments from Lake Braya Sø in Greenland [11]. The separations were carried out using HPLC-APCI-MS equipped with Ag-DMT column at 25°C. In these chromatograms, 2a: $C_{38:2}$Et, 2b: $C_{37:2}$Me, 3a: $C_{38:3}$Et and $C_{39:3}$Et, 3b: $C_{37:3}$Me and $C_{38:3}$Me, 4a: $C_{38:4}$Et and $C_{39:4}$Et, 4b: $C_{37:4}$Me and $C_{38:4}$Me. $C_{38:2}$Me/Et refers to methyl/ethyl straight chain ketones with 38 carbon atoms and 2 C=C double bonds, and ditto. Peaks with asterisks are unknown molecules in the sediment samples.

3.5. Influence of temperature and comparison of thermodynamic properties between Ag-DMT and Ag-MP

Silver thiolate stationary phases display unusual thermodynamic behaviors compared with (cation-exchange) silver ion stationary phases with which analytes were more retained at higher temperature [37,42,56,57]. For example, retention time increased from 13.8 to 20.4 min for methyl ester of $C_{22:6}$ docosahexaenoic acid, and from 12.6 to 28.2 min for LnLnLn TAG with commercially available ChromSpher silver ion HPLC columns when temperature increased from 10 to 40°C [42]. On the other hand, retention factor of each FAEE peak decreases for both Ag-MP and Ag-DMT stationary phases from 15 to 35°C (Fig. S3), suggesting the adsorption of FAEEs on silver-thiolate stationary phases is an exothermic process. A decrease in resolution for pairs of FAEEs with different unsaturation degrees is observed in Ag-MP (e.g., $R_s = 1.3 \rightarrow 1.0$ between mono-unsaturated peak 1 and di-unsaturated peak 2, Fig. S4a) and Ag-DMT (e.g., $R_s = 7.3 \rightarrow 4.4$ between mono-unsaturated peak 1a and di-unsaturated peak 2a, Fig. S4b) from 15 to 35°C. Notably, the degree of resolution decrease varies for different pairs of FAEEs. For example, the resolution for Ag-DMT between tetra-unsaturated peak 4a and penta-unsaturated peak 5a only decreases by 2% ($R_s = 5.0 \rightarrow 4.9$) from 15 to 35°C (Fig. S4b). The longer retentions and higher resolutions at lower temperature observed with silver-thiolate stationary phase suggest that temperature is an important factor in controlling the separations.

For (cation-exchange) silver ion stationary phases, the endothermic adsorptions observed are unusual and haven't been fully understood [37,42,56,57]. One explanation is that besides analytes, acetonitrile or acetone could also form complexes with silver sites in silver ion columns [42]. The stability of such silver-solvent complexes decreases with increasing temperature, thus allowing stronger interaction between silver ions and analytes at higher temperature. For our silver-thiolate stationary phases, the surface silver sites have significantly weaker interaction with unsaturated molecules compared with silver ions in (cation-exchange) silver ion stationary phases [5,6]. Therefore, such solvent effect may be weaker too, leading to exothermic behaviors observed for analytes with silver-thiolate stationary phases.

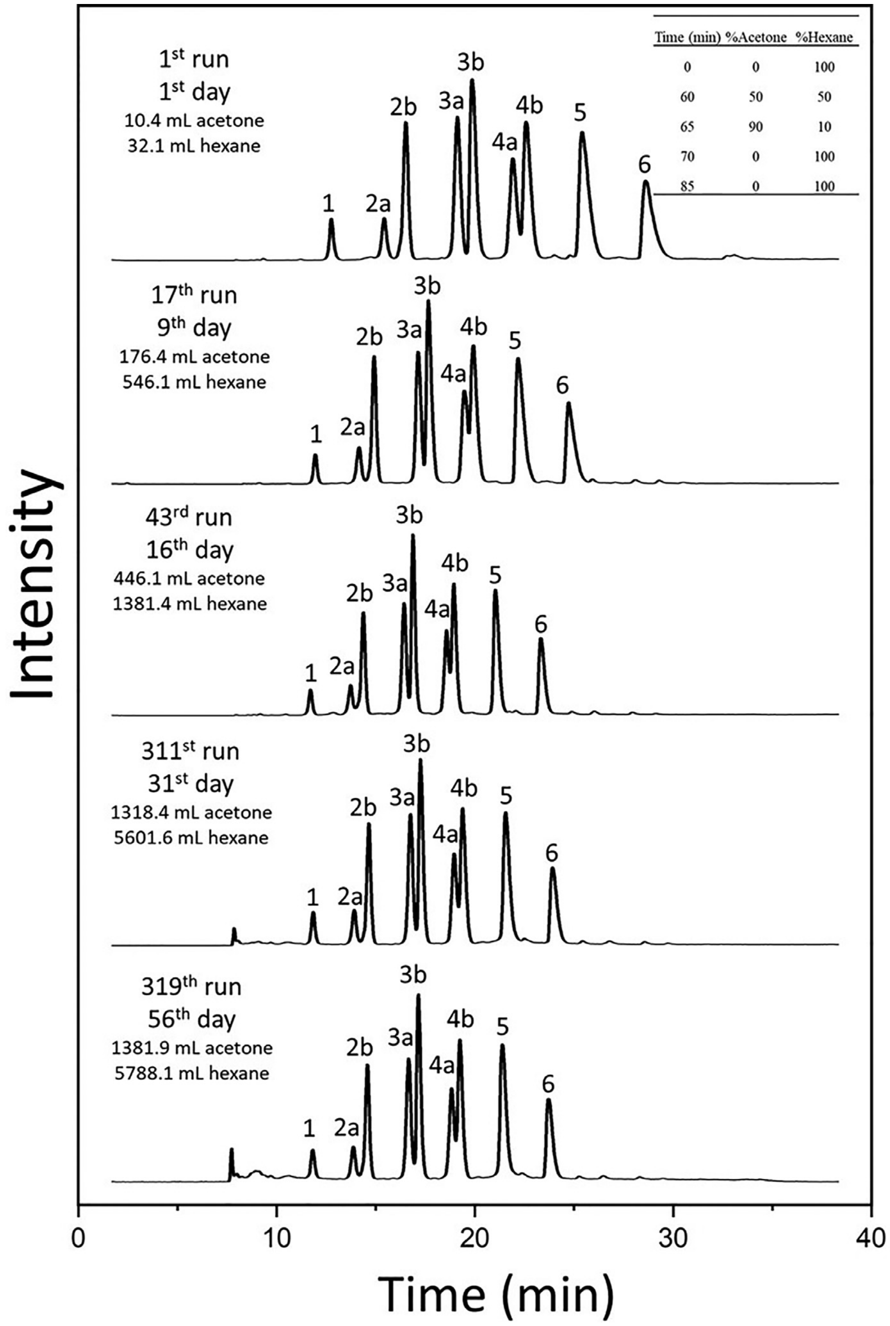

Time (min)	%Acetone	%Hexane
0	0	100
60	50	50
65	90	10
70	0	100
85	0	100

Fig. 5. Examples of total ion chromatograms of sesame seed oil over 319 chromatographic runs. The separations were carried out using HPLC-APCI-MS equipped with Ag-DMT column. All samples were eluted with mobile phases composed of acetone and hexane (total volumes of acetone and hexane used are listed on the figure). Column temperatures ranged from 15 to 35°C for samples analyzed with sesame seed oil analyzed at 25°C. Peak assignments of TAGs in chromatograms remain same as previously demonstrated in Fig. 2b.

Van't Hoff plots are established based on the retention factors of FAEEs from 15 to 35°C (Eq. (2)), which provide a basic understanding of the adsorption process and a theoretical explanation for our observed differences in separation efficiencies between Ag-MP and Ag-DMT. Importantly, we observe excellent linear correlations between $\ln(k)$ and $\frac{1}{T}$ for polyunsaturated FAEEs (FAEEs contain two or more double bonds) in both columns ($R^2 > 0.99$), suggesting the interaction mechanism remains little changed from 15 to 35°C. However, the linear correlation is not observed for saturated and mono-unsaturated FAEEs (Fig. 6a-b, Table S3, Table S4). Such phenomenon might be related to the significant contribution of multiple interactions (e.g., interactions between double bonds and silver sites, alkyl chains and dimercaptotriazine groups/silanol groups) on the retention of saturated and mono-unsaturated FAEEs, while these interactions are not equally influenced by temperature [21]. For polyunsaturated FAEEs, however, their retentions are mainly determined by the interaction strength between double bonds and silver sites in silver-thiolate stationary phases: thus, a linear correlation is observed.

Differences in van't Hoff plots for Ag-MP and Ag-DMT suggest that these two stationary phases have different enthalpy changes and entropy changes during the adsorption of FAEEs (Fig. 6a-b). Enthalpy change (ΔH) could be calculated based on the slope of van't Hoff plots (Eq. (2), Fig. 6c). With increasing number of

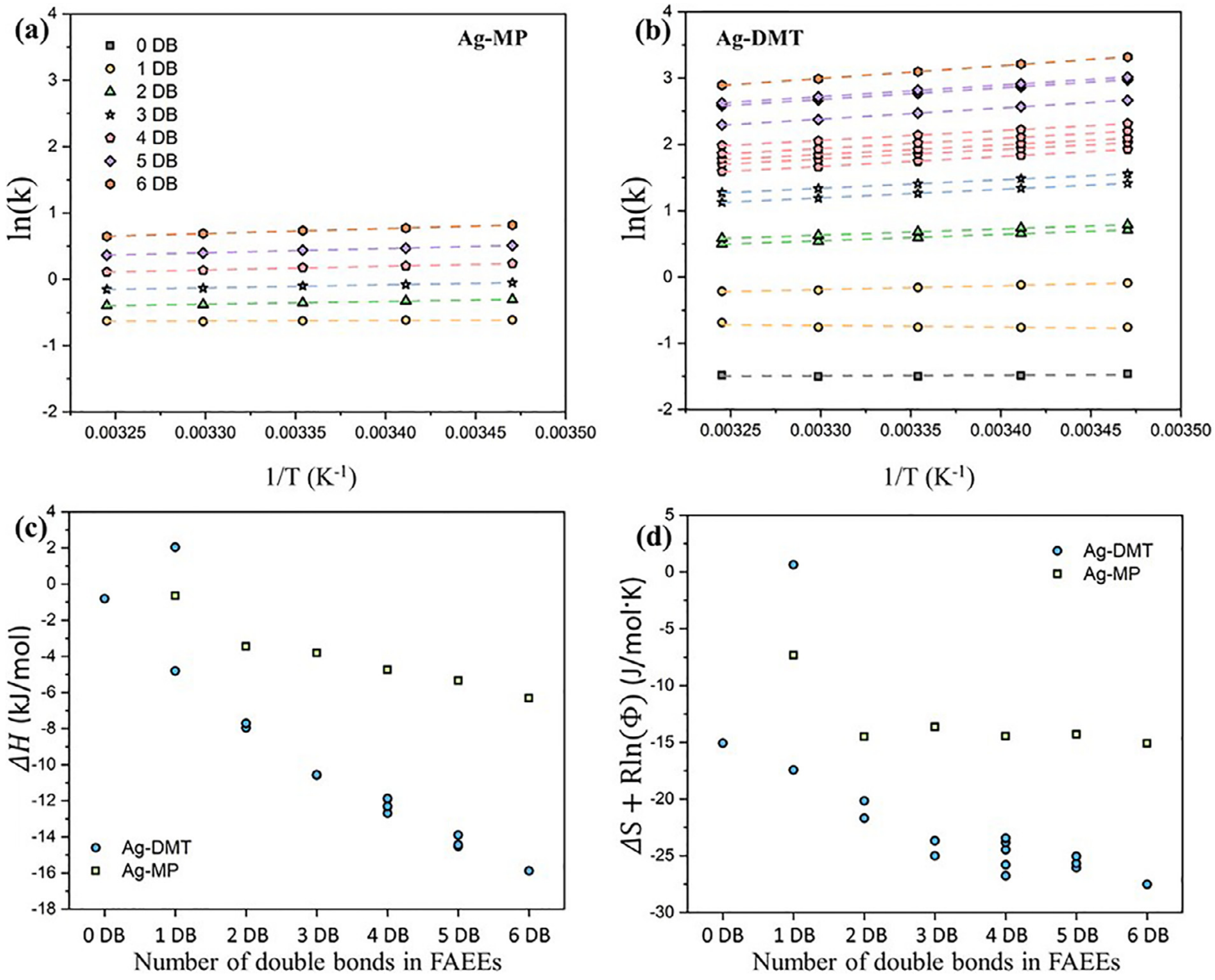

Fig. 6. Van't Hoff plots of FAEEs from 15 to 35°C. The analyses were carried out using HPLC-APCI-MS equipped with (a) Ag-MP and (b) Ag-DMT columns. Isocratic elution with 95% hexane and 5% acetone was used. The separation took approximately 20 minutes for Ag-MP and 60 minutes for Ag-DMT. Correlations between number of double bonds in FAEEs and (c) ΔH^0 and (d) $\Delta S + Rln(\Phi)$ for Ag-MP and Ag-DMT were thus studied. The first peak of FAEEs separated with Ag-MP contained both saturated and mono-unsaturated FAEEs. Mono-unsaturated FAEEs were the dominant components based on mass spectra and separation results using Ag-DMT. Therefore, we treated the first peak as mono-unsaturated FAEEs in the subsequent calculations for Ag-MP.

double bonds, ΔH increases correspondingly for both columns (Fig. 6c). A larger enthalpy change during adsorption process is observed for Ag-DMT than Ag-MP (e.g., for penta-unsaturated FAEEs, $\Delta H = -5.3\ kJ/mol$ for Ag-MP and average $\Delta H = -14.3\ kJ/mol$ for Ag-DMT), indicating a stronger interaction between unsaturated molecules and Ag-DMT stationary phase. Such stronger interaction of Ag-DMT than Ag-MP may originate from the stronger electron-withdrawing effect of DMT group and subsequent stronger coordination between unsaturated bonds and more positively charged silver sites [5]. From the intercept of van't Hoff plots, the sum of ΔS and $Rln(\Phi)$ could be calculated (Eq. (2), Fig. 6d). If phase ratios for Ag-MP and Ag-DMT are similar, $|\Delta S^0|$ would be larger with Ag-DMT than with Ag-MP. This would suggest that the formation of silver complexes on the surface of Ag-DMT with FAEEs molecules has greater order. A decrease of ΔS values is observed from mono- (and saturated) to di-unsaturated FAEEs for Ag-MP stationary phase, or from saturated to tetra-unsaturated FAEEs for Ag-DMT stationary phase (Fig. 6d). Such phenomenon might be related to the single silver site available to FAEEs on each MP group, whereas there are two silver sites on each DMT group and more double bonds in FAEEs could thus interact closely with Ag-DMT stationary phase.

Differences in entropy ($\Delta\Delta S^0$) and enthalpy ($\Delta\Delta H^0$) changes determine the selectivity for pairs of molecules examined (Eq. (3)), with positive values of $\Delta\Delta S^0$ and $\Delta\Delta H^0$ leading to high selectivity. For Ag-DMT stationary phase, higher selectivity and larger $\Delta\Delta H^0$ values ($\Delta\Delta H^0 > 0$) are observed than Ag-MP for all pairs of FAEEs that vary in unsaturation degrees (Table S5, Table S6). Notably, larger $|\Delta\Delta S^0|$ values ($\Delta\Delta S^0 < 0$) are also obtained with Ag-DMT, which partially offset the positive contribution of $\Delta\Delta H^0$ to the selectivity. This suggests $\Delta\Delta H^0$, instead of $\Delta\Delta S^0$, is the key factor that contributes to the higher selectivity in Ag-DMT stationary phase.

3.6. Theoretical calculations of the binding enthalpy between ethylene and silver site on silver thiolate bond, and bond-dissociation energy of silver thiolate (-S-Ag) bond for Ag-MP and Ag-DMT in gas phase

During DFT calculations of Ag-DMT, two conformations with different spatial orientations of -S-Ag bonds are considered through rotating C-S bonds: in conformation 1, both Ag atoms are in the position that only nears one sulfur atom (Ag-DMT-1, Fig. S5b); in conformation 2, both Ag atoms are in the position that is between two sulfur atoms (Ag-DMT-2, Fig. S5c). Binding enthalpies of ethylene are similar for these two conformations (-15.79 kcal/mol for Ag-DMT-1 and -15.87 kcal/mol for Ag-DMT-2, Table 1). On the other hand, free silver ion has the largest ethylene binding enthalpy in gas phase (-34.13 kcal/mol), followed by Ag-

Table. 1
DFT calculations of the binding enthalpy between ethylene and silver site on silver thiolate bond, and bond-dissociation energy of silver thiolate (-S-Ag) bond for Ag-MP and Ag-DMT in gas phase. Calculations were performed using B3LYP with LANL2DZ basis [15,1,18].

Molecule	Binding Energy/(kcal/mol)	Dissociation Energy/(kcal/mol)
Ag^+	-34.13	-
Ag-MP	-14.63	185.53
Ag-DMT-1[1]	-15.79	163.07
Ag-DMT-2[2]	-15.87	150.11

[1] : Conformation that both Ag atoms are in the position that only nears one sulfur atom (Fig. S5b).

[2] : Conformation that both Ag atoms are in the position that is between two sulfur atoms (Fig. S5c).

DMT (-15.83 kcal/mol on average) and smallest binding enthalpy in Ag-MP (-14.63 kcal/mol). The calculated order of ethylene binding enthalpy suggests that the interaction between Ag-DMT and unsaturated molecules is stronger than that of Ag-MP, but weaker than that of silver ion column. These calculations are consistent with the reported separation of unsaturated model compounds on flash columns with these three stationary phases [5], and our observations in the separation of TAGs and FAEEs. Difference in the theoretical binding enthalpy of ethylene (~8.2%) between Ag-MP and Ag-DMT is much smaller than the calculated enthalpy difference of unsaturated FAEEs based on van't Hoff plots (ΔH with Ag-DMT is on average ~2 times higher than ΔH with Ag-MP), suggesting the influence of solvent effect as well as more complex interaction mechanisms between unsaturated FAEEs and silver-thiolate stationary phases.

The bond-dissociation energy of -S-Ag bond into $-S^-$ and Ag^+ in gas phase is smaller in Ag-DMT (156.59 kcal/mol) than in Ag-MP (185.53 kcal/mol) (Table 1). The weaker interaction towards unsaturated bonds and higher bond-dissociation energy of -S-Ag bond in Ag-MP suggest that silver sites in Ag-MP are more stable than those in Ag-DMT. Notably, a higher bond-dissociation energy of -S-Ag bond is obtained in Ag-DMT-1 (163.07 kcal/mol) than Ag-DMT-2 (150.11 kcal/mol), which might relate to a stronger interaction between spatially adjacent N atom and Ag atom in Ag-DMT-1 than in Ag-DMT-2.

4. Conclusions

The new Ag-DMT stationary phase displays higher retention factors, peak capacities and resolutions in the separation of a variety of unsaturated compounds than our previously developed Ag-MP stationary phase. In the case of fish oil separation, Ag-DMT eliminates HPA and DPA impurities from EPA (HPA and DPA coeluted with EPA in our previous test of Ag-MP separations). In the separation of $C_{18:1}$ FAME mixtures, Ag-DMT affords high resolution for *cis*- and *trans*-isomers as well as Δ^6/Δ^9 positional isomers. Ag-DMT also provides excellent resolution for methyl and ethyl alkenones from geological samples. Besides the separation based on characteristics of double bonds (number, position, geometry), FAEEs/TAGs of different chain lengths and alkenones with methyl and ethyl substitutions are also separated by Ag-DMT stationary phase, suggesting strong influence of van der Waals force and steric effects. Ag-DMT shows high stability and repeatability in the separation of TAGs over 319 runs. Differences in separation performances for different compounds between Ag-MP and Ag-DMT suggest that modification of functional groups carrying thiol groups could lead to diverse silver-thiolate stationary phases with different desired separation properties.

Based on van't Hoff plots derived from the separation of FAEEs, Ag-DMT has larger enthalpy changes during the interaction with unsaturated FAEEs than Ag-MP does. This difference can be explained by the stronger electron-withdrawing effect of DMT group. The stronger interaction with unsaturated molecules in Ag-DMT than Ag-MP is further corroborated by DFT calculations using ethylene as the model compound.

Declaration of Competing Interest

The authors declare that they have no known competing financial interests or personal relationships that could have appeared to influence the work reported in this paper.

CRediT authorship contribution statement

Sian Liao: Data curtion, Investigation, Writing – original draft, Formal analysis, Software. **James T. Dillon:** Resources, Investigation, Conceptualization. **Cancan Huang:** Investigation, Formal analysis, Software. **Ewerton Santos:** Investigation. **Yongsong Huang:** Conceptualization, Supervision, Writing – review & editing.

Acknowledgments

This research was supported by the NSF grants to Y.H. (EAR-1122749, PLR-1503846, EAR-1502455, EAR-1762431). Theoretical calculations were performed using resources of the Center for Computation and Visualization supported by NSF Grant No. ACI-1548562. We are also grateful for the comments from three anonymous reviewers, which helped us improve the manuscript.

Supplementary materials

Supplementary material associated with this article can be found, in the online version, at doi:10.1016/j.chroma.2021.462122.

References

[1] L.J. Morris, Separations of lipids by silver ion chromatography, J. Lipid Res. 7 (1966) 717–732.
[2] B. DeVries, Quantitative separations of lipid materials by column chromatography on silica impregnated with silver nitrate, Chem. Ind. 24 (1962) 1049–1050.
[3] B. Nikolova-Damyanova, Retention of lipids in silver ion high-performance liquid chromatography: facts and assumptions, J. Chromatogr. A 1216 (2009) 1815–1824.
[4] S. Momchilova, B. Nikolova-Damyanova, Stationary phases for silver ion chromatography of lipids: preparation and properties, J. Sep. Sci. 26 (2003) 261–270.
[5] J.C. Aponte, J.T. Dillon, R. Tarozo, Y. Huang, Separation of unsaturated organic compounds using silver-thiolate chromatographic material, J. Chromatogr. A 1240 (2012) 83–89.
[6] J.T. Dillon, J.C. Aponte, R. Tarozo, Y. Huang, Efficient liquid chromatographic analysis of mono-, di-, and triglycerols using silver thiolate stationary phase, J. Chromatogr. A 1240 (2012) 90–95.
[7] J.T. Dillon, J.C. Aponte, R. Tarozo, Y. Huang, Purification of omega-3 polyunsaturated fatty acids from fish oil using silver-thiolate chromatographic material and high performance liquid chromatography, J. Chromatogr. A 1312 (2013) 18–25.
[8] J.T. Dillon, W.M. Longo, Y. Zhang, R. Torozo, Y. Huang, Identification of double-bond positions in isomeric alkenones from a lacustrine haptophyte, Rapid Commun. Mass Spectrom. 30 (2016) 112–118.
[9] Y. Huang, J.C. Aponte, R. Tarozo, J. Dillon, Functionalized chromatographic materials and methods of making and using therefor, U.S. Patent 10,549,255 (2020).
[10] L.N. Mander, C.M. Williams, Chromatography with silver nitrate: part 2, Tetrahedron 72 (2016) 1133–1150.
[11] W.J. D'Andrea, Y. Huang, Long chain alkenones in Greenland lake sediments: low $\delta^{13}C$ values and exceptional abundance, Org. Geochem. 36 (2005) 1234–1241.
[12] J.M. Lo, H. Sakamoto, Comparison of the acid combinations in microwave-assisted digestion of marine sediments for heavy metal analyses, Anal. Sci. 21 (2005) 1181–1184.
[13] S.D. Fazio, S.A. Tomellini, S.H. Hsu, J.B. Crowther, T.V. Raglione, T.R. Floyd, R.A. Hartwick, Chemical characterization of bonded stationary phases for high--performance liquid chromatography using hydrofluoric acid digestion and gas chromatography, Anal. Chem. 57 (1985) 1559–1564.
[14] F. Aureli, M. Ciprotti, M. D'Amato, E. do Nascimento da Silva, S. Nisi, D. Passeri, A. Sorbo, A. Raggi, M. Rossi, F. Cubadda, Determination of total silicon and SiO_2 particles using an ICP-MS based analytical platform for toxicokinetic studies of synthetic amorphous silica, Nanomaterials 10 (2020) 888.

[15] P.J. Stephens, F.J. Devlin, C.F. Chabalowski, M.J. Frisch, *Ab initio* calculation of vibrational absorption and circular dichroism spectra using density functional force fields, J. Phys. Chem. 98 (1994) 11623–11627.

[16] P.J. Hay, W.R. Wadt, *Ab initio* effective core potentials for molecular calculations. Potentials for the transition metal atoms Sc to Hg, J. Chem. Phys. 82 (1985) 270–283.

[17] M. Frisch, G. Trucks, H.B. Schlegel, G.E. Scuseria, M.A. Robb, J.R. Cheeseman, G. Scalmani, V. Barone, B. Mennucci, G. Petersson, et al., Gaussian 09, Revision A.01, Gaussian Inc., Wallingford, CT, 2009.

[18] J. Kaneti, L.C. de Smet, R. Boom, H. Zuilhof, E.J. Sudhölter, Computational probes into the basis of silver ion chromatography. II. Silver (I)−olefin complexes, J. Phys. Chem. A 106 (2002) 11197–11204.

[19] M.D. Hanwell, D.E. Curtis, D.C. Lonie, T. Vandermeersch, E. Zurek, G.R. Hutchison, Avogadro: an advanced semantic chemical editor, visualization, and analysis platform, J. Chemin. 4 (2012) 17.

[20] J.W. Dolan, L.R. Snyder, N.M. Djordjevic, D.W. Hill, T.J. Waeghe, Reversed-phase liquid chromatographic separation of complex samples by optimizing temperature and gradient time: I. peak capacity limitations, J. Chromatogr. A 857 (1999) 1–20.

[21] M. Tanase, A. Soare, V. David, S.C. Moldoveanu, Sources of nonlinear van't Hoff temperature dependence in high-performance liquid chromatography, ACS omega 4 (2019) 19808–19817.

[22] A. Péter, G. Török, D.W. Armstrong, G. Tóth, D. Tourwé, Effect of temperature on retention of enantiomers of β-methyl amino acids on a teicoplanin chiral stationary phase, J. Chromatogr. A 828 (1998) 177–190.

[23] J. Flieger, H. Trębacz, M. Pizoń, A. Kowalska, A. Szczęsna, T. Plech, High--performance liquid chromatography thermodynamic study of new potential antiepileptic compounds on a cholesterol column using isocratic elution with methanol/water and acetonitrile/water eluent systems, J. Sep. Sci. 40 (2017) 4176–4190.

[24] T.L. Chester, J.W. Coym, Effect of phase ratio on van't Hoff analysis in reversed-phase liquid chromatography, and phase-ratio-independent estimation of transfer enthalpy, J. Chromatogr. A 1003 (2003) 101–111.

[25] S. Momchilova, B. Nikolova-Damyanova, Silver ion HPLC of *p*-methoxyphenacyl derivatives of unsaturated fatty acids. II. Chain length vs. double bond position, J. Liq. Chromatogr. Rel. Technol. 23 (2000) 2317–2325.

[26] R.O. Adlof, Normal-phase separation effects with lipids on a silver ion high--performance liquid chromatography column, J. Chromatogr. A 764 (1997) 337–340.

[27] O.V. Sayanova, J.A. Napier, Eicosapentaenoic acid: biosynthetic routes and the potential for synthesis in transgenic plants, Phytochemistry 65 (2004) 147–158.

[28] H.E. Bays, C.M. Ballantyne, J.J. Kastelein, J.L. Isaacsohn, R.A. Braeckman, P.N. Soni, Eicosapentaenoic acid ethyl ester (AMR101) therapy in patients with very high triglyceride levels (from the multi-center, plAcebo-controlled, randomized, double-blINd, 12-week study with an open-label extension [MARINE] trial), Am. J. Cardiol. 108 (2011) 682–690.

[29] M. Peet, K.S. Vaddadi, Highly purified ethyl EPA and other EPA derivatives, U.S. Patent 8,188,146 (2012).

[30] E.H. Belarbi, E. Molina, Y. Chisti, A process for high yield and scaleable recovery of high purity eicosapentaenoic acid esters from microalgae and fish oil, Enzyme Microb. Technol. 26 (2000) 516–529.

[31] B.G. Nordestgaard, A. Varbo, Triglycerides and cardiovascular disease, Lancet 384 (2014) 626–635.

[32] M. Buchgraber, F. Ulberth, H. Emons, E. Anklam, Triacylglycerol profiling by using chromatographic techniques, Eur. J. Lipid Sci. Technol. 106 (2004) 621–648.

[33] N.K. Andrikopoulos, Triglyceride species compositions of common edible vegetable oils and methods used for their identification and quantification, Food Rev. Int. 18 (2002) 71–102.

[34] S. Indelicato, D. Bongiorno, R. Pitonzo, V. Di Stefano, V. Calabrese, S. Indelicato, G. Avellone, Triacylglycerols in edible oils: Determination, characterization, quantitation, chemometric approach and evaluation of adulterations, J. Chromatogr. A 1515 (2017) 1–16.

[35] K. Aitzetmüller, M. Grönheim, Separation of highly unsaturated triacylglycerols by reversed-phase HPLC with short wavelength UV detection, J. High Resolut. Chromatogr. 15 (1992) 219–226.

[36] E. Salivaras, A. McCurdy, Detection of olive oil adulteration with canola oil from triacylglycerol analysis by reversed-phase high-performance liquid chromatography, J. Am. Oil Chem. Soc. 69 (1992) 935–938.

[37] M. Lísa, H. Velínská, M. Holčapek, Regioisomeric characterization of triacylglycerols using silver-ion HPLC/MS and randomization synthesis of standards, Anal. Chem. 81 (2009) 3903–3910.

[38] M.B. Macher, A. Holmqvist, Triacylglycerol analysis of partially hydrogenated vegetable oils by silver ion HPLC, J. Sep. Sci. 24 (2001) 179–185.

[39] M. Buchgraber, F. Ulberth, E. Anklam, Comparison of HPLC and GLC techniques for the determination of the triglyceride profile of cocoa butter, J. Agric. Food Chem. 48 (2000) 3359–3363.

[40] K. Ben Arfa, M. de Person, D. Hmida, J. Bleton, S. Boukhchina, A. Tchapla, S. Heron, F. Moussa, UHPLC-APCI-MS profiling of triacylglycerols in vegetable oils-application to the analysis of four North African sesame seed varieties, Food Anal. Methods 10 (2017) 2827–2838.

[41] P. Dugo, O. Favoino, P.Q. Tranchida, G. Dugo, L. Mondello, Off-line coupling of non-aqueous reversed-phase and silver ion high-performance liquid chromatography–mass spectrometry for the characterization of rice oil triacylglycerol positional isomers, J. Chromatogr. A 1041 (2004) 135–142.

[42] R. Adlof, G. List, Analysis of triglyceride isomers by silver-ion high-performance liquid chromatography: effect of column temperature on retention times, J. Chromatogr. A 1046 (2004) 109–113.

[43] R.V. Denev, I.S. Kuzmanova, S.M. Momchilova, B.M. Nikolova-Damyanova, Resolution and quantification of isomeric fatty acids by silver ion HPLC: fatty acid composition of aniseed oil (*Pimpinella anisum, Apiaceae*), J. AOAC Int. 94 (2011) 4–8.

[44] R. Adlof, T. Lamm, Fractionation of *cis*- and *trans*-oleic, linoleic, and conjugated linoleic fatty acid methyl esters by silver ion high-performance liquid chromatography, J. Chromatogr. A 799 (1998) 329–332.

[45] B. Nikolova-Damyanova, W.W. Christie, B. Herslöf, Mechanistic aspects of fatty acid retention in silver ion chromatography, J. Chromatogr. A 749 (1996) 47–54.

[46] M. Dołowy, A. Pyka, Chromatographic methods in the separation of long-chain mono-and polyunsaturated fatty acids, J. Chem. 2015 (2015) 1–20.

[47] P. Delmonte, A.-R.F. Kia, Q. Hu, J.I. Rader, Review of methods for preparation and gas chromatographic separation of *trans* and *cis* reference fatty acids, J. AOAC Int. 92 (2009) 1310–1326.

[48] P. Delmonte, A. Kataoka, B. Corl, D. Bauman, M.P. Yurawecz, Relative retention order of all isomers of *cis*/*trans* conjugated linoleic acid FAME from the 6, 8- to 13, 15-positions using silver ion HPLC with two elution systems, Lipids 40 (2005) 509–514.

[49] W.W. Christie, G. Dobson, R.O. Adlof, A practical guide to the isolation, analysis and identification of conjugated linoleic acid, Lipids 42 (2007) 1073–1084.

[50] C. Cruz-Hernandez, Z. Deng, J. Zhou, A.R. Hill, M.P. Yurawecz, P. Delmonte, M.M. Mossoba, M.E. Dugan, J.K. Kramer, Methods for analysis of conjugated linoleic acids and *trans*-18: 1 isomers in dairy fats by using a combination of gas chromatography, silver-ion thin-layer chromatography/gas chromatography, and silver-ion liquid chromatography, J. AOAC Int. 87 (2004) 545–562.

[51] C. Villegas, Y. Zhao, J. Curtis, Two methods for the separation of monounsaturated octadecenoic acid isomers, J. Chromatogr. A 1217 (2010) 775–784.

[52] Y. Zheng, P. Heng, M.H. Conte, R.S. Vachula, Y. Huang, Systematic chemotaxonomic profiling and novel paleotemperature indices based on alkenones and alkenoates: potential for disentangling mixed species input, Org. Geochem. 128 (2019) 26–41.

[53] S. Liao, Y. Yao, L. Wang, K.J. Wang, L. Amaral-Zettler, W.M. Longo, Y. Huang, C_{41} methyl and C_{42} ethyl alkenones are biomarkers for group II isochrysidales, Org. Geochem. 147 (2020) 104081.

[54] A. Huynh, B. Maktabi, C.M. Reddy, G.W. O'Neil, M. Chandler, G. Baki, Evaluation of alkenones, a renewably sourced, plant-derived wax as a structuring agent for lipsticks, Int. J. Cosm. Sci. 42 (2020) 146–155.

[55] G.W. O'Neil, A.R. Culler, J.R. Williams, N.P. Burlow, G.J. Gilbert, C.A. Carmichael, R.K. Nelson, R.F. Swarthout, C.M. Reddy, Production of jet fuel range hydrocarbons as a coproduct of algal biodiesel by butenolysis of long-chain alkenones, Energy Fuel 29 (2015) 922–930.

[56] R. Adlof, Analysis of triacylglycerol and fatty acid isomers by low-temperature silver-ion high performance liquid chromatography with acetonitrile in hexane as solvent: limitations of the methodology, J. Chromatogr. A 1148 (2007) 256–259.

[57] M. Lísa, R. Denev, M. Holčapek, Retention behavior of isomeric triacylglycerols in silver-ion HPLC: effects of mobile phase composition and temperature, J. Sep. Sci. 36 (2013) 2888–2900.